# Low-spin states and the non-observation of a proposed 2202-keV, $0^{+}$ isomer in $^{68}$Ni

C. J. Chiara, R. Broda, W. B. Walters, R. V. F. Janssens, M. Albers, M. Alcorta, P. F. Bertone, M. P. Carpenter, C. R. Hoffman, T. Lauritsen, A. M. Rogers, D. Seweryniak, S. Zhu, F. G. Kondev, B. Fornal, W. Królas, J. Wrzesiński, N. Larson, S. N. Liddick, C. Prokop, S. Suchyta, H. M. David, and D. T. Doherty

# Low-spin states and the non-observation of a proposed 2202-keV, $0^+$ isomer in $^{68}$Ni

C. J. Chiara,[1,2] R. Broda,[3] W. B. Walters,[1] R. V. F. Janssens,[2] M. Albers,[2] M. Alcorta,[2]
P. F. Bertone,[2] M. P. Carpenter,[2] C. R. Hoffman,[2] T. Lauritsen,[2] A. M. Rogers,[2,*]
D. Seweryniak,[2] S. Zhu,[2] F. G. Kondev,[4] B. Fornal,[3] W. Królas,[3] J. Wrzesiński,[3]
N. Larson,[5] S. N. Liddick,[5] C. Prokop,[5] S. Suchyta,[5] H. M. David,[6,2] and D. T. Doherty[6,2]

[1]*Department of Chemistry and Biochemistry, University of Maryland, College Park, Maryland 20742, USA*
[2]*Physics Division, Argonne National Laboratory, Argonne, Illinois 60439, USA*
[3]*Niewodniczański Institute of Nuclear Physics PAN, PL-31342 Kraków, Poland*
[4]*Nuclear Engineering Division, Argonne National Laboratory, Argonne, Illinois 60439, USA*
[5]*National Superconducting Cyclotron Laboratory and Department of Chemistry,*
*Michigan State University, East Lansing, Michigan 48824, USA*
[6]*School of Physics and Astronomy, University of Edinburgh, Edinburgh, EH9 3JZ, UK*
(Dated: October 1, 2012)

The low-spin level scheme of $^{68}$Ni was investigated with the Gammasphere array following reactions between a $^{70}$Zn beam and $^{238}$U, $^{208}$Pb, and $^{197}$Au targets. Spin assignments for some states have been verified through $\gamma$-ray angular correlations, including the $0^+$ assignment for the 2511-keV level. Two previously unknown states at 3302 and 3405 keV have been identified. No evidence was found for a recently reported 216-ns, $0^+$ isomer at 2202 keV that was attributed to a proton two-particle, two-hole intruder configuration, despite experimental conditions similar to those used in the measurement reporting its discovery.

PACS numbers: 23.20.Lv, 23.20.En, 21.10.Hw, 27.50.+e

Nuclei in the $^{68}$Ni region have proven to be an important testing ground for nucleon-nucleon interactions underlying shell model (SM) calculations. Early studies of $^{68}$Ni indicated that it possibly had doubly-magic character, with a closed proton shell at $Z = 28$ and neutron subshell at $N = 40$ [1, 2]. Subsequent work in the region revealed the transitory nature of the latter shell gap, as the magicity was found not to persist in other $N \approx 40$ nuclei [3–6] and some theoretical efforts such as those in Refs. [7–10] have called into question the $N = 40$ magicity in $^{68}$Ni itself. The weakening of the $N = 40$ shell gap, as well as the generation of collectivity in this region, have drawn considerable attention to the influence of neutron excitations across the $N = 40$ and $N = 50$ shell gaps into the $g_{9/2}$ and $d_{5/2}$ single-particle states, respectively, and of excitations across the $Z = 28$ gap, e.g. Refs. [7, 11–13]. The investigation of intruder states—those with configurations based upon orbitals originating from across a shell gap—can provide valuable insight into the size of such gaps and their variation with nucleon number. Results on the odd-$Z$ isotopes $^{64,66}$Mn [14], $^{65-68}$Co [15–17], and $^{67,69,71}$Cu [18–20] have demonstrated the role of a single proton intruder in the structure of nuclei on either side of the $Z = 28$ shell gap.

More recently, an isomeric state attributed to a two-particle, two-hole ($2p2h$) proton intruder configuration in even-$Z$ $^{68}$Ni was proposed in Ref. [21]. Reproducing these experimental results provides a challenge to modern SM calculations which, in addition, must also account for the reordering of orbitals within the $fp$ shell due mostly to effects of the tensor force [22]. Thus, further experimental information in this region is important to test the most recent interactions and single-particle energies. In turn, these developments serve as a basis for descriptions of more neutron-rich nuclei, including $^{78}$Ni and beyond.

Prior to this work, ten states below 3.5 MeV had been proposed in $^{68}$Ni [1, 2, 21, 23–25]. Four of the lowest five states have been assigned spin and parity $I^\pi = 0^+$, including the recently proposed $2p2h$ isomer [2, 21, 23]. Significant experimental uncertainties remain for some of these levels: several have only tentative $I^\pi$ assignments and the energy of the first excited $0^+$ state is not well known (1770(30) keV [2]). Furthermore, despite those studies which were sensitive to isomeric decays in $^{68}$Ni ($\beta$ decay [23], fragmentation reactions [21, 26, 27]), only one measurement has claimed the observation of a 2202-keV $0^+$ isomer. This level is of importance, as its location would provide a stringent test of pairing and proton-neutron correlations [21]. Therefore, we set out to address these deficiencies in our knowledge of the low-energy spectrum of $^{68}$Ni. In addition, the experimental setups and analysis techniques for studies of multinucleon-transfer reactions have demonstrated sensitivity to both prompt and delayed deexcitations in neutron-rich nuclei (see, for example, Refs. [18, 28–30]), including the ability to perform coincidence measurements across isomers with lifetimes of up to several microseconds [6]. This ability presents the opportunity to search for prompt $\gamma$ rays feeding the reported $2p2h$ isomer.

This paper concentrates on the low-spin states in $^{68}$Ni, with significant attention given to the proposed proton-$2p2h$ isomer. Despite experimental conditions similar to

TABLE I: Details of the experimental running conditions. The *trigger* column indicates the minimum number of coincident $\gamma$ rays required to define an event. The number of such events for each reaction is given in the last column. Typical beam intensities of 0.2 to 0.4 pnA were used.

| $E_{beam}$ [MeV] | target | trigger | duration [h] | # events |
|---|---|---|---|---|
| 430 | $^{197}$Au | $\gamma^{\geq 3}$ | 68 | $2.1 \times 10^9$ |
| 440 | $^{197}$Au | $\gamma^{\geq 2}$ | 12 | $3.8 \times 10^8$ |
| 440 | $^{238}$U | $\gamma^{\geq 2}$ | 8 | $4.1 \times 10^8$ |
| 440 | $^{208}$Pb | $\gamma^{\geq 2}$ | 32 | $1.3 \times 10^9$ |
| 440 | $^{208}$Pb | $\gamma^{\geq 3}$ | 64 | $2.2 \times 10^9$ |

those used in Ref. [21], no evidence for the isomer was found. Higher-spin structure of $^{68}$Ni is discussed in a forthcoming paper [24].

Excited states in $^{68}$Ni were populated through multi-nucleon transfer reactions using 430- and 440-MeV $^{70}$Zn beams provided by the ATLAS facility at Argonne National Laboratory. The beam was directed onto heavy, neutron-rich targets located at the center of the Gammasphere array of 100 Compton-suppressed Ge detectors [31]. Reactions with three different thick targets were investigated: $^{238}$U ($\sim$55 mg/cm$^2$), $^{208}$Pb ($\sim$44 mg/cm$^2$), and $^{197}$Au ($\sim$50 mg/cm$^2$). The targets were angled at 27° with respect to the vertical, and were thick enough to stop all reaction products. One in five beam bursts was allowed to reach the target, resulting in beam pulses of $\sim$0.3-ns width every 412 ns. Several combinations of beam energy, target, and trigger condition were explored, as seen in Table I.

The beam structure allowed $\gamma$ rays to be designated as prompt (P), if detected within a 50-ns window centered on the beam burst, or delayed (D), for those $\gamma$ rays emitted within either of the $\sim$400-ns regions between the prompt and two successive beam bursts. In events for which DD coincidence relationships were considered, a further requirement that the two delayed $\gamma$ rays were detected within 50 ns of each other was imposed, effectively reducing the contribution from random events. The data were unfolded into triple-$\gamma$ coincidence events and the energies $E_\gamma$ sorted into three-dimensional histograms (*cubes*) according to their prompt or delayed nature—i.e., into PPP, PPD, PDD, and DDD cubes. The data were similarly sorted into double-$\gamma$ histograms (*matrices*) with PP, PD, or DD coincidence requirements. The programs LEVIT8R and ESCL8R, part of the RAD-WARE analysis package [32], were used to project double- and single-gated background-subtracted spectra from the cubes and matrices, respectively. Such spectra were examined to confirm and possibly add to the low-spin level scheme of $^{68}$Ni and to search for coincident transitions associated with the proposed isomeric $0^+$ state.

An important characteristic of multinucleon transfer reactions is the simultaneous excitation of the partner nuclei. Typically, following transfer of a number of nucleons, several neutrons are evaporated [1, 33, 34]. Thus, in removing two protons from the $^{70}$Zn projectile and transferring them to the $^{208}$Pb target, for example, transitions in $^{210}$Po and several lighter Po isotopes are observed in coincidence with excitations in $^{68}$Ni.

In order to perform an angular-correlation (AC) analysis, a set of 11 DD matrices was created from the $^{70}$Zn $+ \, ^{208}$Pb data in the same manner as described in Sec. IV of Ref. [18]. For the set of PP counterparts to these AC matrices, an additional requirement of a third, delayed $\gamma$ ray originating from one of the cross-coincident nuclei $^{208-210}$Po ($E_\gamma = 660, 686; 782, 545; 245, 1182$ keV [35–38]) was imposed to provide cleaner spectra. No specific angle was required for the delayed $\gamma$ ray. This additional requirement reduces the overall number of counts in the peaks, so several angles were combined leading to the five average angles 20.3°, 37.5°, 55.4°, 71.4°, and 85.2° for the gated-AC analysis. In both the delayed and prompt analyses, a gate was placed on the 2033-keV, $2^+ \to 0^+$ transition in $^{68}$Ni [1] and the AC function $W(\psi)$ was determined for the correlated transition in $^{68}$Ni. As is customary, prompt $\gamma$ rays were assumed to be of dipole ($E1$ or $M1$), quadrupole ($E2$), or mixed ($M1/E2$) character.

A coincidence spectrum from the $^{70}$Zn $+ \, ^{208}$Pb PPD cube, created from the sum of gates on the prompt 2033-keV transition in $^{68}$Ni and either of the delayed 1182- and 245-keV lines in the cross-coincident nucleus $^{210}$Po (located below sequential 98.9-, 42.6-, and 1.53-ns isomers [39, 40]), is presented in Fig. 1(a). The three prompt $\gamma$ rays at 478, 710, and 1114 keV are known to feed the 2033-keV, $2_1^+$ state [1, 23]. An additional line at 1269 keV, not in coincidence with the other three, has been identified in the present work as depopulating a level at 3302 keV. This $\gamma$ ray had not been previously observed in either $\beta$ decay or deep-inelastic reactions. All of these lines are in cross coincidence with $^{208,209}$Po as well, confirming their placement in $^{68}$Ni. A level at 3405 keV has also been found to decay by parallel 662- and 258-keV transitions, in coincidence with the 710- and 1114-keV $\gamma$ rays, respectively. Spectra illustrating these coincidence relations in the $^{70}$Zn $+ \, ^{208}$Pb PPP cube are given in Fig. 1(b,c). The 662-keV transition may be the same as the one observed, but not placed, by Mueller *et al.* [23] following $\beta$ decay into levels of $^{68}$Ni.

In the DD matrices, a gate on the 2033-keV $\gamma$ ray reveals quite prominently the expected 814-keV decay from the 2847-keV $5^-$ isomer [1]. The 0.86-ms half-life of this state is much longer than the width of the delayed time window in this analysis and, thus, the $\gamma$ ray appears uncorrelated with the corresponding prompt beam pulses, just as $\gamma$ rays following $\beta$ decay would (see, for example, Ref. [29]). Figure 2(a) provides this coincidence spectrum from a gate on the $^{70}$Zn $+ \, ^{238}$U DD matrix, but those from the $^{208}$Pb and $^{197}$Au targets produce similar results. These prompt and delayed transitions are indicated in the partial level scheme of Fig. 3.

The AC of the $814-2033$-keV pair was measured in the delayed AC matrices, while those of the 478-, 710-, 1114-
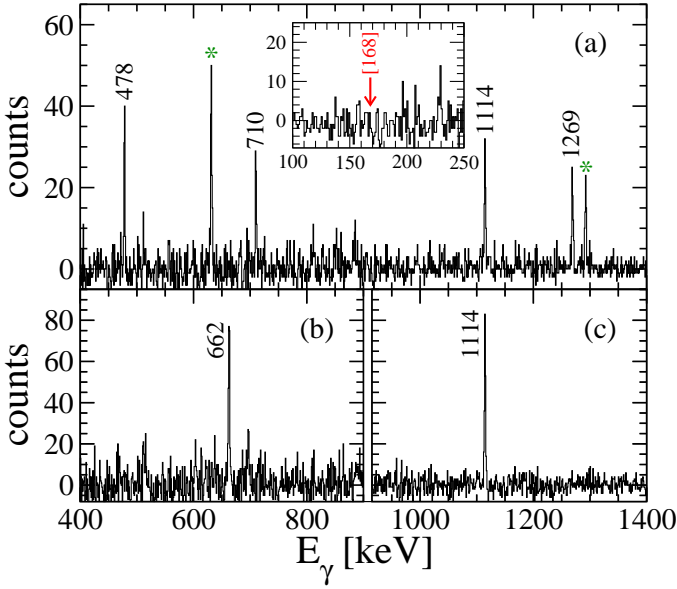
FIG. 1: (Color online) Background-subtracted coincidence spectra from the $^{70}$Zn + $^{208}$Pb data. (a) Double gate in the PPD cube on the prompt 2033-keV transition in $^{68}$Ni and the delayed 1182- and 245-keV transitions in the partner nucleus $^{210}$Po. Panels (b) and (c) are double gated in the PPP cube on the 2033-keV transition and on the (b) 710- and (c) 258-keV $\gamma$ rays. Peaks labelled by their energies in keV belong to $^{68}$Ni; those marked with an asterisk lie above the isomer in $^{210}$Po. The inset in (a) provides an expanded region of this spectrum around 168 keV.



FIG. 2: (Color online) Background-subtracted coincidence spectra from the $^{70}$Zn + $^{238}$U DD matrix, gated on the (a) 2033-keV $\gamma$ ray in $^{68}$Ni and (b) the 1871-keV $^{69}$Cu transition. Peaks labelled by their energies in keV indicate the $\gamma$ rays observed following isomeric decay in the respective nuclei. The sum of the spectra gated on the 2033-keV line in the DD matrices for all three targets is given in the inset to panel (a), expanded around the expected location of the 168-keV $\gamma$ ray. See text for details.

, and 1269-keV transitions with respect to the 2033-keV gate were determined from the prompt, gated-AC matrices. The results are plotted in Fig. 4 in comparison with the theoretical AC curves for different spin hypotheses. The spin and parity of the 2847-keV isomer were previously established as $5^-$ [1, 25]; the AC for the 814-keV transition measured here agrees with this assignment [Fig. 4(a)]. The 1114-keV transition [Fig. 4(b)] is found to be consistent ($\chi_\nu^2 < 1$) with an $E2$ multipolarity, although $\Delta I = 0$ or 1 $M1/E2$ assignments (with best fit $\delta = -2.2$ or 0.4, respectively) also agree with the data. The AC fit with a $2^+$ initial state has the lowest $\chi_\nu^2$, but this is rejected in favor of a $4^+$ assignment for the 3147-keV state based on the large mixing ratio that would be required for a $2^+ \to 2^+$ transition, AC results from another reaction [24], and this state being a member of the yrast cascade fed by the 23-ns $8^+$ isomer [19, 24]. The AC for the 710-keV transition [Fig. 4(c)] is in better agreement with a $\Delta I = 0$ $M1/E2$ multipolarity (best fit $\delta = -1.5$) than with $E2$ or $\Delta I = 1$ $M1/E2$ assignments. The resulting $2^+$ assignment for the 2743-keV level verifies the tentative spin from Ref. [23]. The presence of the 2743-keV crossover transition supports this assertion.

The upsloping AC of the 1269-keV transition [Fig. 4(d)] rules out an $E2$ assignment, whereas the data are well reproduced by a $\Delta I = 1$ $E1$ or $M1/E2$ ($\delta \approx 0$)
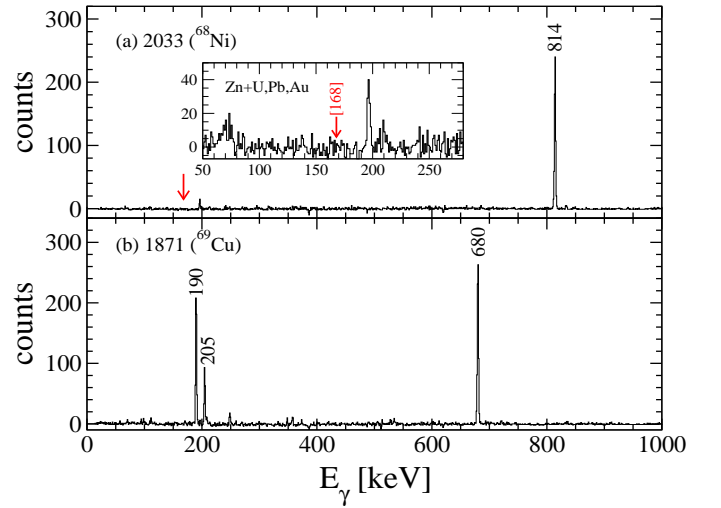
or a $\Delta I = 0$ $M1/E2$ ($\delta = 0.4$) assignment, with corresponding initial values $I^\pi = 3^-$, $3^+$, or $2^+$, respectively. A ($2^+$ or $4^+$) state was identified at 3280(50) keV in the $^{70}$Zn($^{14}$C,$^{16}$O) quasi-elastic transfer reaction of Ref. [41]; if this level is the same as the 3302-keV state observed here, the spin and parity would then be fixed at $2^+$. However, in view of the large discrepancy in energy for the $2_1^+$ level in Ref. [41] [2200(30) keV compared to 2033 keV], this assignment is unlikely. Instead, the energy of this level appears to be consistent with the positions of the $3^-$ levels in the lighter Ni isotopes [24] and the 3302-keV state is tentatively assigned $I^\pi = (3^-)$. Such a level would not likely be directly populated in the $\beta$ decay of either the ($1^+$) or ($7^-$) isomers in $^{68}$Co [16, 23], nor would much intensity reach it in studies involving reactions populating yrast states at higher spins, possibly explaining why this state had not been observed previously. The assignment for this state is discussed in more detail in Ref. [24].

Finally, the 2511-keV state was inferred to have tentative $I^\pi = (0^+)$ quantum numbers by Mueller et al. [23], based on an assumed $0^+ \to 0^+$ decay yielding 511-keV $\gamma$ rays. The AC of the $478 - 2033$-keV cascade parallel to this proposed $E0$ decay is shown in Fig. 4(e). The distinctive shape of this curve is characteristic of a $0^+ \to 2^+ \to 0^+$ sequence and is in disagreement with other possible initial spin values. Thus, the $0^+$ assignment for the 2511-keV level is confirmed.
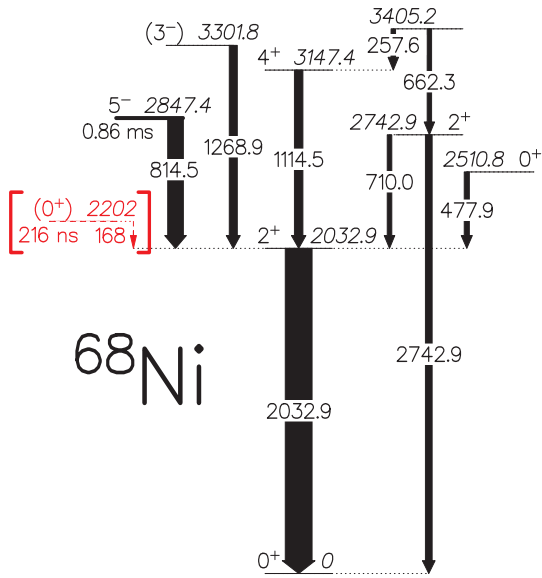
An attempt was made to determine more accurately

FIG. 3: (Color online) Partial, low-spin level scheme of $^{68}$Ni from the present study. The 168-keV isomeric transition proposed in Ref. [21] was *not* observed in this work, but is indicated for reference.

the energy of the 1770(30)-keV, $0_2^+$ state by searching for prompt transitions feeding it. Such transitions are expected to be in coincidence with a delayed $[t_{1/2}(0_2^+) = 270$ ns] 511-keV $\gamma$ ray resulting from the $0_2^+ \to 0_1^+$ decay by internal pair creation, as well as with prompt transitions either depopulating a higher-lying state in $^{68}$Ni (in both the $^{208}$Pb and $^{197}$Au PPD data sets) or in the cross-coincident nucleus $^{199}$Tl ($^{197}$Au PPD cube only). No candidate transition could be identified.

Dijon *et al.* [21] assigned a newly identified 168-keV transition in $^{68}$Ni as depopulating a proposed $0^+$ state at 2202 keV with a half-life of $t_{1/2} = 216^{+66}_{-50}$ ns. This transition would directly feed the 2033-keV, $2_1^+$ state (see Fig. 3). The absence of the 2033-keV line in the delayed $\gamma$-ray data in Ref. [21] was attributed to the rather low efficiency of their focal-plane Ge array above 2 MeV. In a search of data from deep-inelastic reactions between $^{48}$Ca, $^{64}$Ni, and $^{76}$Ge beams and a $^{238}$U target [24], using experimental setups similar to the current work, the expected 168-keV transition was not observed in a coincidence gate placed on the 2033-keV, $2_1^+ \to 0_1^+$ transition. An upper limit of 0.4% was obtained for the ratio of the yields of the 2202- and 2847-keV isomers within the delayed time window, as determined by the areas of peaks at 168 keV (limit only) and at 814 keV in the 2033-keV gate, corrected for $\gamma$-ray efficiency. As with the proposed $168 - 2033$-keV sequence [21], the well established $814 - 2033$-keV coincidence is also a two-$\gamma$ cascade depopulating an isomer (the 0.86-ms $5^-$ state), demonstrating the sensitivity of these experiments to low-multiplicity events. Arguably, however, the deep-inelastic reactions discussed in Ref. [24] would favor population of yrast

states in $^{68}$Ni and may not have much yield for an excited $0^+$ state. To appropriately test the findings presented in Ref. [21], experimental conditions that are expected to populate states in $^{68}$Ni similarly to the previous work are desirable.

The 6.3-MeV/$A$ $^{70}$Zn + $^{238}$U reaction used in the current study is equivalent in center-of-mass excitation to the reverse-kinematics 6.3-MeV/$A$ $^{238}$U + $^{70}$Zn reaction used in the work by Dijon *et al.* [21]. It is, therefore, expected that the *same* excited states of $^{68}$Ni would be populated in both cases. Furthermore, similar states should also be populated in the $^{70}$Zn + $^{208}$Pb and $^{70}$Zn + $^{197}$Au reactions employed in the current study, as the transfer of exactly two protons from beam to target nuclei can contribute significantly to the overall $^{68}$Ni yield in each case, leading to population of non-yrast states such as the 2511-keV, $0^+$ state mentioned earlier. Indeed, the $2p$ transfer mechanism may be expected to enhance the population of a proton $2p2h$ level. Thus, spectra from all three data sets can be considered for comparison with the results of Ref. [21]. The sensitivity to isomers, the observation of another excited $0^+$ state in $^{68}$Ni at 2511 keV, and high coincidence efficiencies in the present work imply that this experimental setup is well suited for investigating the presence of the proposed 2202-keV, $0^+$ isomer.

All combinations of prompt and delayed coincidence cubes and matrices in the current data set were investigated for evidence of a 168-keV $\gamma$ ray associated with $^{68}$Ni. No such transition could be identified. In particular, a gate on the 2033-keV transition in the $^{70}$Zn + $^{238}$U DD matrix produced the coincidence spectrum in Fig. 2(a), where a peak at 168 keV would be expected according to the level scheme proposed in Ref. [21]. As with the deep-inelastic reactions of Ref. [24], the measured ratio of yields of a peak at 168 keV and of the 814-keV $\gamma$ ray has a similarly small upper limit of 0.5%. Summing the spectra gated on the 2033-keV transition in the DD matrices for all three targets produces the spectrum in the inset of Fig. 2(a); it is clear that no peak is present at 168 keV with any statistical significance in all the available data. Although the reported half-life was quoted as 216 ns [21], for completeness we also show the spectrum around 168 keV in the prompt data (from reactions with the $^{208}$Pb target) in the inset of Fig. 1(a); again, there is no evidence for a 168-keV peak.

To provide a more direct comparison between our results and those in Ref. [21], it is important to estimate what the expected yield *should* be for the suggested $0^+$ isomer in the present data. Dijon *et al.* do not explicitly provide measured intensities, but these can be inferred semi-quantitatively by comparing the $^{68}$Ni and $^{69}$Cu mass spectra presented in Fig. 2 of Ref. [21]. The spectrum for the former was generated by a gate on the 168-keV $\gamma$ ray and, for the latter, on unspecified lines in $^{69}$Cu, which would presumably include at least the 190- and 680-keV transitions following decay of the 0.36-$\mu$s $13/2^+$ isomer [19]. Taking into account the relative
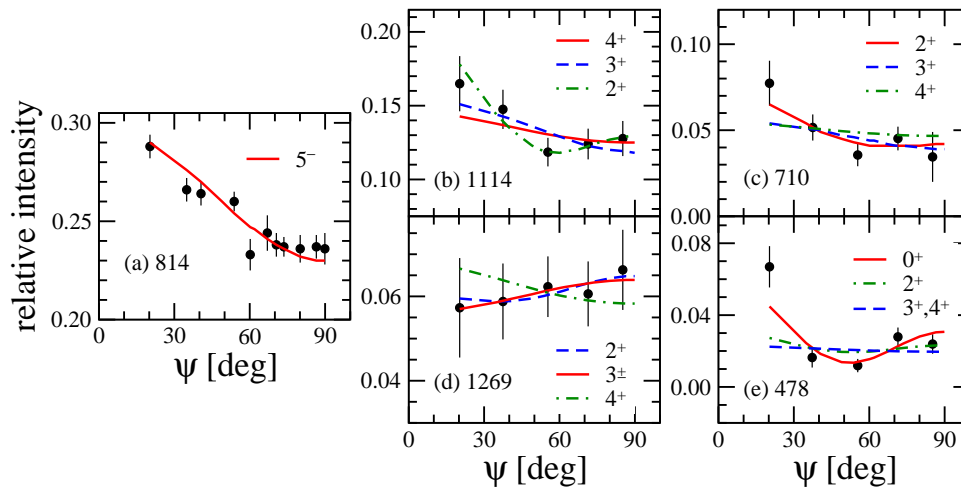
FIG. 4: (Color online) Angular correlations of $\gamma$ rays feeding the $2_1^+$ state in $^{68}$Ni, relative to the 2033-keV gating transition. Panel (a) is for the 814-keV transition in the DD data. Panels (b-e) show the 1114-, 710-, 1269-, and 478-keV ACs, respectively, from the PP matrices gated on delayed Po lines (see text for details). The data points are compared with curves calculated for $I_i^\pi \to 2^+ \to 0^+$ ACs, where the values of $I_i^\pi$ are noted in the legends. For mixed $M1/E2$ transitions, the curves represent the best-fit values of the mixing ratio $\delta$. In each panel, the solid (red) line corresponds to the adopted assignment. In (d) and (e), two ACs that are very similar are drawn with a single line.

detector efficiencies and widths of time gates in both experiments (estimated, for Ref. [21]), the population of the proposed 2202-keV isomer in our $^{70}$Zn + $^{238}$U data should be comparable to that of the $13/2^+$ isomer in $^{69}$Cu. Specifically, in the delayed (DD) coincidence spectra, the area of the 168-keV peak in the 2033-keV gate [Fig. 2(a)] should be at least 70% of the area of the 190-keV peak in the spectrum gated on the 1871-keV $\gamma$ ray in $^{69}$Cu [Fig. 2(b)]. In our data, however, the upper limit for a peak at 168 keV is two orders of magnitude smaller than this estimate, in clear disagreement with the placement of the 168-keV $\gamma$ ray feeding the 2033-keV $2_1^+$ level in $^{68}$Ni. It should be reemphasized that this peak is absent not only in the $^{70}$Zn + $^{238}$U data, but also in the longer runs with the $^{208}$Pb and $^{197}$Au targets. Furthermore, the fact that the decay of the 0.36-$\mu$s $13/2^+$ isomer in $^{69}$Cu is clearly observed [Fig. 2(b)] indicates the suitability of the present experimental setup for isomer detection.

From this analysis, it is concluded that a 168-keV $\gamma$ ray cannot be placed as proposed in Ref. [21], and that there is no conclusive evidence for a 2202-keV, $0^+$ isomer in $^{68}$Ni. Such a transition has not been observed in coincidence with the 2033-keV, $2^+ \to 0^+$ decay in either our delayed or prompt spectra. Furthermore, there is also no evidence in the data for coincidences between a 168-keV transition and other known lines in $^{68}$Ni. These observations present an interesting conundrum as to the origin of the line in Ref. [21], given the sensitivity of the setup to identifying the $Z$ and $A$ of recoils on an event-by-event basis. One possibility is that there is a 168-keV isomeric transition in $^{68}$Ni that is *not* in coincidence (within $\sim$50 ns) with the 2033-keV $\gamma$ ray. This could occur if, for example, the purported isomer decays

directly to the 2847-keV, $5^-$ isomer or to the $0_2^+$ level at 1770(30) keV [2]. If the former is the case, the fact that the decay has not been located and connected to the negative-parity levels in studies following $\beta$ decay or deep-inelastic reactions would be surprising. The latter scenario, on the other hand, would have the unexpected implication that there would be another $2^+$ level lying below the known one at 2033 keV; this level would then be the yrast $2^+$ state and would have been expected to receive significant feeding. In the absence of additional information about the experimental details of Ref. [21], it is difficult to explain the possible origins of the 168-keV $\gamma$ ray.

In summary, low-lying excited states in $^{68}$Ni have been studied in reactions between a $^{70}$Zn beam and $^{238}$U, $^{208}$Pb, and $^{197}$Au targets. The usage of thick targets and beam pulsing provided sensitivity to both prompt and delayed decays. Several $\gamma$-ray angular correlations were measured, confirming previous spin-parity assignments including that of the 2511-keV, $0^+$ state. A ($3^-$) level at 3302 keV and a second level at 3405 keV have been identified. Particular attention was devoted to searching for the decay of the proton-$2p2h$, 2202-keV, $0^+$ isomer proposed in Ref. [21]. No evidence for such an intruder state was observed in the present study. Given the impact such a state would have on understanding the structure of nuclei in the $^{68}$Ni region, more conclusive evidence of its location is required.

[1] R. Broda *et al.*, Phys. Rev. Lett. **74**, 868 (1995).

[2] M. Bernas *et al.*, Phys. Lett. **B 113**, 279 (1982).

[3] M. Hannawald *et al.*, Phys. Rev. Lett. **82**, 1391 (1999).

[4] C. Guénaut *et al.*, Phys. Rev. C **75**, 044303 (2007).

[5] A. Gade *et al.*, Phys. Rev. C **81**, 051304(R) (2010).

[6] S. Zhu *et al.*, Phys. Rev. C **85**, 034336 (2012).

[7] O. Sorlin *et al.*, Phys. Rev. Lett. **88**, 092501 (2002).

[8] K. Langanke, J. Terasaki, F. Nowacki, D. J. Dean, and W. Nazarewicz, Phys. Rev. C **67**, 044314 (2003).

[9] L. Gaudefroy *et al.*, Phys. Rev. C **80**, 064313 (2009).

[10] H. Nakada, Phys. Rev. C **81**, 051302(R) (2010).

[11] K. Sieja and F. Nowacki, Phys. Rev. C **81**, 061303(R) (2010).

[12] S. M. Lenzi, F. Nowacki, A. Poves, and K. Sieja, Phys. Rev. C **82**, 054301 (2010).

[13] P. C. Srivastava, Mod. Phys. Lett. A **27**, 1250061 (2012).

[14] S. N. Liddick *et al.*, Phys. Rev. C **84**, 061305 (2011).

[15] D. Pauwels *et al.*, Phys. Rev. C **78**, 041307(R) (2008).

[16] S. N. Liddick *et al.*, Phys. Rev. C **85**, 014328 (2012).

[17] D. Pauwels *et al.*, Phys. Rev. C **79**, 044309 (2009).

[18] C. J. Chiara *et al.*, Phys. Rev. C **85**, 024309 (2012).

[19] T. Ishii *et al.*, Phys. Rev. Lett. **84**, 39 (2000).

[20] A. M. Oros-Peusquens and P. F. Mantica, Nucl. Phys. **A669**, 81 (2000).

[21] A. Dijon *et al.*, Phys. Rev. C **85**, 031301(R) (2012).

[22] T. Otsuka *et al.*, Phys. Rev. Lett. **95**, 232502 (2005).

[23] W. F. Mueller *et al.*, Phys. Rev. C **61**, 054308 (2000).

[24] R. Broda *et al.* (to be published).

[25] E. A. McCutchan, Nucl. Data Sheets **113**, 1735 (2012).

[26] J. M. Daugas, Ph.D. thesis, University of Caen (1999).

[27] J. M. Daugas *et al.*, Phys. Rev. C **81**, 034304 (2010).

[28] I. Stefanescu *et al.*, Phys. Rev. C **79**, 034319 (2009).

[29] N. Hoteling *et al.*, Phys. Rev. C **82**, 044305 (2010).

[30] C. J. Chiara *et al.*, Phys. Rev. C **82**, 054313 (2010).

[31] I. Y. Lee, Nucl. Phys. **A520**, 641c (1990).

[32] D. C. Radford, Nucl. Instrum. Methods Phys. Res. A **361**, 297 (1995).

[33] B. Fornal *et al.*, Phys. Rev. C **72**, 044315 (2005).

[34] R. Broda, J. Phys. G: Nucl. Part. Phys. **32**, R151 (2006).

[35] A. R. Poletti, G. D. Dracoulis, A. P. Byrne, A. E. Stuchbery, B. Fabricius, T. Kibédi, and P. M. Davidson, Nucl. Phys. **A615**, 95 (1997).

[36] A. R. Poletti, G. D. Dracoulis, A. P. Byrne, A. E. Stuchbery, B. Fabricius, T. Kibédi, and P. M. Davidson, Nucl. Phys. **A665**, 318 (2000).

[37] L. G. Mann, K. H. Maier, A. Aprahamian, J. A. Becker, D. J. Decman, E. A. Henry, R. A. Meyer, N. Roy, W. Stöffl, and G. L. Struble, Phys. Rev. C **38**, 74 (1988).

[38] Evaluated Nuclear Structure Data File (ENSDF) [http://www.nndc.bnl.gov/ensdf].

[39] O. Häusser, T. K. Alexander, J. R. Beene, E. D. Earle, A. B. McDonald, F. C. Khanna, and I. S. Towner, Nucl. Phys. **A273**, 253 (1976).

[40] E. Browne, Nucl. Data Sheets **99**, 649 (2003).

[41] M. Girod, Ph. Dessagne, M. Bernas, M. Langevin, F. Pougheon, and P. Roussel, Phys. Rev. C **37**, 2600 (1988).